2024 IEEE 63rd Conference on Decision and Control (CDC)
December 16-19, 2024. MiCo, Milan, Italy

Sampled-data distributed control of mixed traffic flow with ACC-equipped vehicles

Hanxu Zhao, Jingyuan Zhan, and Liguo Zhang

Abstract— **This paper studies the sampled-data distributed control problem for mixed traffic flow described by the Aw-Rascle-Zhang (ARZ) model, which consists of both manual and adaptive cruise control-equipped (ACC-equipped) vehicles. A group of stationary sensing devices provides spatially averaged state measurements over the sampling spatial intervals, and then the sampled-data distributed controller is designed as the time-gap setting of ACC-equipped vehicles based on the state measurements sampled in space and time. The closed-loop system is re-organized into an equivalent system containing a continuous time control loop and spatio-temporal sampling errors. Then sufficient conditions for ensuring exponential stability of the mixed traffic flow system are developed in terms of matrix inequalities, by employing the Lyapunov function method along with Wirtinger's and Jensen's inequalities in H^1-norm. Finally, the effectiveness of the proposed method is verified by numerical simulations.**

I. INTRODUCTION

The evolution of macroscopic traffic state can usually be described by hyperbolic partial differential equation (PDE) systems [1], [2], and extensive studies have been devoted to the boundary control of hyperbolic PDE-based traffic flow models [3], [4], [5]. With the emergence of automated and connected vehicles, the approach to regulating the dynamic of traffic flow by designing the real-time setting of ACC-equipped vehicles is attracting more attention. It has been proven that properly manipulating ACC-equipped vehicles is effective for stabilizing traffic flow dynamics [6], [7]. For instance, the exponential and convective stability were guaranteed for a freeway traffic flow by designing the time-gap of ACC-equipped vehicles in [8].

As another relevant subject of this paper, sampled-data control has been extensively applied in modern control systems since the controller can be implemented by digital technology. Although sampled-data control problems of ODE systems have been widely investigated [9], there are few counterpart studies on PDE systems [10], [11]. An event-based boundary controller was presented for a linear hyperbolic system of conservation laws by defining two event-triggering conditions in [12], and then the global exponential stability and well-posedness of the closed-system were proved. In [13], the sampled-data control problem was considered for a class of linear hyperbolic systems with state measurements sampled in space and time via the Lyapunov-Razumikhin approach.

To the best of authors' knowledge, the sampled-data distributed control for hyperbolic PDEs in mixed traffic flow based on ARZ model has not been addressed yet. Motivated by the aforementioned discussion, we consider the problem of sampled-data distributed control for the mixed traffic flow in this paper. The ARZ model is utilized to describe the mixed traffic flow which consists of both manual and ACC-equipped vehicles. Considering the connected feature of the ACC-equipped vehicles, the time-gap setting of ACC-equipped vehicles is designed based on the state measurements sampled both in time and space provided by a group of stationary sensing devices. The exponential stability analysis in H^1-norm is presented by using the Lyapunov function method with the application of Wirtinger's and Jensen's inequalities.

Notation: R, R^n and $R^{n\times m}$ denote the set of real numbers, n-order vectors and $n\times m$-order matrices, respectively. For a matrix A, $A^\top$ denotes the transpose matrix of A, and trace(A) denotes the trace of A. $A > (<)\ 0$ denotes that A is a positive (negative) definite matrix. $\mathtt{diag}\{a_1,...,a_n\}$ is the diagonal matrix with $a_i \in R, i=1,...,n$. $\mathbb{N}$ is the set of nonnegative integers from 0 to infinity. For a partitioned symmetric matrix, symbol $*$ stands for the symmetric blocks. Given a function $g:[0,L]\to R^n$, we define its H^1-norm as $\|g\|_{H^1((0,L);R^n)} = \sqrt{\int_0^L(|g|^2+|g_x|^2)dx}$, where $|\cdot|$ is the Euclidean norm in R^n.

II. MIXED TRAFFIC FLOW WITH ACC-EQUIPPED VEHICLES

A. Mixed traffic flow model

Consider the mixed traffic flow consisting of manual and ACC-equipped vehicles as shown in Fig. 1, where the percentage of ACC-equipped vehicles with respect to total vehicles is $\alpha\in[0,1]$. $\tau_{\mathtt{acc}}$, $\tau_{\mathtt{m}} > 0$ denote the time constants of ACC-equipped and manual vehicles, respectively. Let $\rho(x,t)$ and $v(x,t)$ represent the traffic density and the average speed, respectively, which are defined in $x\in[0,L]$ for position and $t\in[0,+\infty)$ for time. L is the length of the road. The macroscopic mixed traffic flow dynamic is described by the ARZ model, i.e., the following second-order

This work was supported by the National Natural Science Foundation of China (Nos. U2233211, 62273014), R&D Program of Beijing Municipal Education Commission (Nos. KZ20231000523, KM202310005032), the Beijing Nova Program (No. 20220484133), and the Beijing Municipal College Faculty Construction Plan for Outstanding Young Talents (No. BPHR202203011).

H. Zhao, J. Zhan and L, Zhang (corresponding author) are with the Faculty of Information Technology, Beijing University of Technology, and with the Beijing Key Laboratory of Computational Intelligence and Intelligent Systems, Beijing, 100124, China. (E-mail: zhaohx@emails.bjut.edu.cn, jyzhan@bjut.edu.cn, zhangliguo@bjut.edu.cn.)

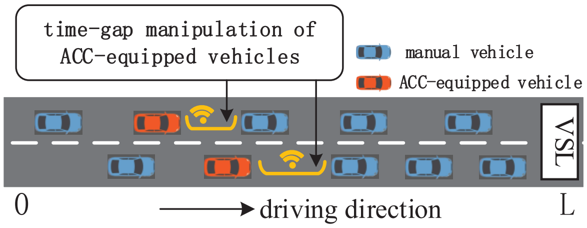

Fig. 1. Time-gap manipulation of ACC-equipped vehicles for the mixed traffic flow.

hyperbolic PDE system of balance law:

$$\begin{cases} \partial_t \rho + \partial_x (v\rho) = 0, \\ \partial_t v + \left(v + \rho \frac{\partial V_{\mathtt{mix}}(\rho, h_{\mathtt{acc}}(x,t))}{\partial_\rho}\right)\partial_x v = \frac{V_{\mathtt{mix}}(\rho, h_{\mathtt{acc}}(x,t)) - v}{\tau_{\mathtt{mix}}}, \end{cases} \tag{1}$$

with $\tau_{\mathtt{mix}} = \frac{1}{\frac{\alpha}{\tau_{\mathtt{acc}}} + \frac{1-\alpha}{\tau_{\mathtt{m}}}}$.

We utilize the following fundamental diagram relation [8]

$$V_{\mathtt{mix}}(\rho, h_{\mathtt{acc}}) = \tau_{\mathtt{mix}}\left(\frac{\alpha}{\tau_{\mathtt{acc}}} V_{\mathtt{acc}}(\rho, h_{\mathtt{acc}}) + \frac{1-\alpha}{\tau_{\mathtt{m}}} V_{\mathtt{m}}(\rho)\right), \tag{2}$$

with

$$V_{\mathtt{acc}}(\rho, h_{\mathtt{acc}}) = \frac{1}{h_{\mathtt{acc}}}\left(\frac{1}{\rho} - D\right), \rho_{\min} < \rho < \frac{1}{D}, \tag{3}$$

$$V_{\mathtt{m}}(\rho) = \frac{1}{h_{\mathtt{m}}}\left(\frac{1}{\rho} - D\right), \rho_{\min} < \rho < \frac{1}{D}, \tag{4}$$

where $D > 0$ is the average effective vehicle length and $\rho_{\min} > 0$ is the lowest density value for which the model is accurate. $h_{\mathtt{m}} > 0$ is the time gap of manual vehicles, and $h_{\mathtt{acc}} > 0$ is the time gap of ACC-equipped vehicles, which is the control input to be designed later.

Substituting (3)-(4) into (2), the fundamental diagram of mixed traffic flow model can be rewritten as

$$V_{\mathtt{mix}}(\rho, h_{\mathtt{acc}}) = \frac{1}{h_{\mathtt{mix}}(h_{\mathtt{acc}})}\left(\frac{1}{\rho} - D\right), \tag{5}$$

where the mixed time gap is

$$h_{\mathtt{mix}}(h_{\mathtt{acc}}) = \frac{\alpha + (1-\alpha)\frac{\tau_{\mathtt{acc}}}{\tau_{\mathtt{m}}}}{\alpha + (1-\alpha)\frac{\tau_{\mathtt{acc}}}{\tau_{\mathtt{m}}}\frac{h_{\mathtt{acc}}}{h_{\mathtt{m}}}} h_{\mathtt{acc}}. \tag{6}$$

At the downstream boundary, a variable speed limit (VSL) device is applied to regulate the traffic dynamic. the driving-out speed $v(L,t)$ could be adjusted based on the density information $\rho(L,t)$ at the downstream boundary, that is,

$$v(L,t) = v^* + k_v(\rho(L,t) - \rho^*), \tag{7}$$

where ρ^*, v^* are the steady states of system (1), and $k_v \in R$ is boundary tuning gain.

Assumption 1: For the mixed traffic flow model (1), we assume that the flux at the upstream boundary is constant, i.e., $\rho(0,t)v(0,t) = q_{in}$, where $q_{in} = \rho^* v^*$ is a constant external inflow.

B. Linearization and diagonalization

Denote $h^*_{\mathtt{acc}}$ as steady-state time gap for ACC-equipped vehicles, which results in the following steady-state mixed time gap

$$h^*_{\mathtt{mix}} = \frac{\alpha + (1-\alpha)\frac{\tau_{\mathtt{acc}}}{\tau_{\mathtt{m}}}}{\alpha + (1-\alpha)\frac{\tau_{\mathtt{acc}}}{\tau_{\mathtt{m}}}\frac{h^*_{\mathtt{acc}}}{h_{\mathtt{m}}}} h^*_{\mathtt{acc}} \tag{8}$$

satisfying $\frac{1}{\rho^*} - D = h^*_{\mathtt{mix}} v^*$.

Define the deviations of the variables $\rho, v, h_{\mathtt{acc}}$ from the steady states $\rho^*, v^*, h^*_{\mathtt{acc}}$ by $\tilde{\rho} = \rho - \rho^*, \tilde{v} = v - v^*, \tilde{h}_{\mathtt{acc}} = h_{\mathtt{acc}} - h^*_{\mathtt{acc}}$, and then the linearized system $(\tilde{\rho}, \tilde{v}, \tilde{h}_{\mathtt{acc}})$ around the steady states is deduced as

$$\begin{cases} \partial_t \tilde{\rho} + v^* \partial_x \tilde{\rho} + \rho^* \partial_x \tilde{v} = 0, \\ \partial_t \tilde{v} - c_4 \partial_x \tilde{v} = -c_1 \tilde{\rho} - c_2 \tilde{v} - c_3 \tilde{h}_{\mathtt{acc}}, \end{cases} \tag{9}$$

where $c_1 = 1/({\rho^*}^2 h^*_{\mathtt{mix}} \tau_{\mathtt{mix}})$, $c_2 = 1/\tau_{\mathtt{mix}}$, $c_3 = (\alpha/\tau_{\mathtt{acc}} {h^*_{\mathtt{acc}}}^2)(1/\rho^* - D)$, $c_4 = D/h^*_{\mathtt{mix}}$.

Based on Assumption 1, we have $(\tilde{\rho}(0,t) + \rho^*)(\tilde{v}(0,t) + v^*) = q_{in}$ at the left boundary $x = 0$. Subtracting the steady condition $\rho^* v^* = q_{in}$, then we obtain

$$\tilde{\rho}(0,t) = -\frac{\rho^*}{v^*}\tilde{v}(0,t). \tag{10}$$

Defining the Riemann coordinate as $\tilde{z} = \tilde{v}$, $\tilde{\omega} = \tilde{\rho} + h^*_{\mathtt{mix}} {\rho^*}^2 \tilde{v}$, then systems (9) could be rewritten in the following diagonal form

$$\begin{cases} \partial_t \tilde{\omega} + v^* \partial_x \tilde{\omega} = -c_2 \tilde{\omega} - h^*_{\mathtt{mix}} {\rho^*}^2 c_3 \tilde{h}_{\mathtt{acc}}, \\ \partial_t \tilde{z} - c_4 \partial_x \tilde{z} = -c_1 \tilde{\omega} - c_3 \tilde{h}_{\mathtt{acc}}, \end{cases} \tag{11}$$

with the boundary conditions

$$\begin{cases} \tilde{\omega}(0,t) = (h^*_{\mathtt{mix}} {\rho^*}^2 - \frac{\rho^*}{v^*})\tilde{z}(0,t), \\ \tilde{z}(L,t) = \frac{k_v}{1 + k_v h^*_{\mathtt{mix}} {\rho^*}^2}\tilde{\omega}(L,t). \end{cases} \tag{12}$$

Let $\xi = [\tilde{\omega}, \tilde{z}]^T$, and then the linearized mixed traffic flow model (11) can be rewritten as

$$\partial_t \xi + \Gamma \partial_x \xi = M\xi - H\tilde{h}_{\mathtt{acc}}, \quad t \in [t_k, t_{k+1}), \tag{13}$$

with $\Gamma = \mathtt{diag}\{v^*, -c_4\}$ and

$$M = \begin{bmatrix} -c_2 & 0 \\ -c_1 & 0 \end{bmatrix}, \; H = \begin{bmatrix} h^*_{\mathtt{mix}} {\rho^*}^2 c_3 \\ c_3 \end{bmatrix}.$$

The input and output of system (13) on the right and the left boundaries can be denoted as $\xi^{in} = [\tilde{\omega}(0,t), \tilde{z}(L,t)]^\top$ and $\xi^{out} = [\tilde{\omega}(L,t), \tilde{z}(0,t)]^\top$. Then the boundary condition of system (13) can be rewritten as

$$\xi^{in} = G\xi^{out}, \tag{14}$$

with

$$G = \begin{bmatrix} 0 & h^*_{\mathtt{mix}} {\rho^*}^2 - \frac{\rho^*}{v^*} \\ \frac{k_v}{1 + k_v h^*_{\mathtt{mix}} {\rho^*}^2} & 0 \end{bmatrix}.$$

Further, we denote the initial condition of system (13) as

$$\xi^0 = \begin{bmatrix} \tilde{\omega}(x,0) \\ \tilde{z}(x,0) \end{bmatrix}. \tag{15}$$

C. Time-gap setting of ACC-equipped vehicles

To regulate the dynamic of mixed traffic flow, we design the time gap of ACC-equipped vehicles based on the spatially averaged state measurements provided by a group of stationary sensing devices.

Following [10], we assume that there are N sensors uniformly distributed over the interval $[0, L]$. $\bar{x}_i, i \in \{0, ..., N-1\}$ denotes the location of sensors, such that $\bar{x}_0 = 0, \bar{x}_i = \bar{x}_{i-1} + \bar{b}$, where $\bar{b} = L/(N-1)$, $i \in \{1, ..., N-1\}$. Each sensor i provides the measurements of state at discrete time instant t_k and at position $\bar{x}_i$. The time sequence $\{t_k\}, k \in \mathbb{N}$ represents the sampling time instants with $0 = t_0 < t_1 < \cdots < t_k$. The sampling time intervals are bounded, i.e., $t_{k+1} - t_k \in (0, h]$, where $h > 0$ is the upper bound.

Based on the spatially sampled state measurements provided by these sensors, the sampling state $(\tilde{\omega}(\bar{x}_i, t_k), \tilde{z}(\bar{x}_i, t_k))$ can be transferred to the controller, and the resulting feedback is implemented to the mixed traffic flow model system through a zero-order holder (ZOH). We then design the time-gap manipulation of ACC-equipped vehicles as

$$h_{\mathtt{acc}}(x,t) = h^*_{\mathtt{acc}} + \sum_{i=0}^{N-1} d_i(x)\big[k_\omega \tilde{\omega}(\bar{x}_i, t_k) + k_z \tilde{z}(\bar{x}_i, t_k)\big], \quad t \in [t_k, t_{k+1}), \tag{16}$$

where $k_\omega, k_z \in R$ are control gains. The shape function $d_i(x)$, which can obtain a linear combination of controllers responsible for each region, is defined as

$$\begin{cases} d_i(x) = 1, & x \in \Psi_i,\ i \in \{0, ..., N-1\}, \\ d_i(x) = 0, & otherwise, \end{cases} \tag{17}$$

with $\Psi_i = [x_i, x_{i+1})$ denoting the interval each sensor charged for and

$$\begin{cases} x_i = \frac{\bar{x}_{i-1} + \bar{x}_i}{2}, & i \in \{1, ..., N-1\}, \\ x_0 = 0,\ x_N = L. \end{cases} \tag{18}$$

The well-posedness and the existence of the classical maximal solutions of $H^1((0, L); R^2)$ of the Cauchy problem (13)-(15) are easily adapted from [13]. The definition of the exponential stability for system (13) under the boundary condition (14) is given hereinafter.

Definition 1: The system (13)-(14) under the time-gap setting of ACC-equipped vehicles (16) is exponentially stable for H^1-norm, if there exist scalars $\epsilon > 0$ and $\chi > 0$ such that, for every $\xi^0 \in H^1((0, L); R^2)$, the solution to the Cauchy problem (13) and (14) satisfies

$$\|\xi(\cdot, t)\|_{H^1((0,L);R^2)} \le \chi e^{-\epsilon t} \|\xi^0\|_{H^1((0,L);R^2)} \tag{19}$$

for all $t \in [0, \infty)$.

In this paper, we aim to derive sufficient conditions for ensuring the exponential stability of the mixed traffic flow system (13)-(14) under time-gap manipulation of ACC-equipped vehicles (16). We then state the main results of this paper in next section.

III. MAIN RESULTS

In this section, we analyze the exponential stability of the mixed traffic flow system (13)-(14) under the time-gap setting of ACC-equipped vehicles (16) in H^1-norm, by re-organizing the closed-loop system into an equivalent system with spatio-temporal sampling errors as well as employing the Lyapunov function method.

Defining the time sampling error $\eta(x,t)$ and the space discretization error $\delta(x, t_k)$ as $\eta(x,t) = \xi(x,t) - \xi(x,t_k)$, $t \in [t_k, t_{k+1})$, and $\delta(x, t_k) = \xi(x, t_k) - \sum_{i=0}^{N-1} d_i(x)\xi(\bar{x}_i, t_k)$, respectively.

According to the above spatio-temporal sampling errors, for $t \in [t_k, t_{k+1})$, the time-gap setting of ACC-equipped vehicles (16) equals to

$$\tilde{h}_{\mathtt{acc}}(x,t) = K\xi(x,t) - K\eta(x,t) - K\delta(x,t_k), \tag{20}$$

with $K = \begin{bmatrix} k_\omega & k_z \end{bmatrix}$. Then the closed-loop system (13)-(14) can be written as

$$\partial_t \xi + \Gamma \partial_x \xi = U\xi + F\eta + F\delta(x, t_k), \tag{21}$$

$$\xi^{in} = G\xi^{out}, \ \ \forall t \in [t_k, t_{k+1}),\ k \in \mathbb{N}, \tag{22}$$

with $U = M - HK$, $F = HK$.

Before giving the main result of this paper, we define some matrices that will be used.

$$M_1 = \begin{bmatrix} -c_2 & 0 \\ 0 & 0 \end{bmatrix},\ H_1 = \begin{bmatrix} h^*_{\mathtt{mix}}\rho^{*2} c_3 k_w & 0 \\ 0 & c_3 k_z \end{bmatrix},$$

$$M_2 = \begin{bmatrix} 0 & 0 \\ -c_1 & 0 \end{bmatrix},\ H_2 = \begin{bmatrix} 0 & h^*_{\mathtt{mix}}\rho^{*2} c_3 k_z \\ c_3 k_w & 0 \end{bmatrix}.$$

For diagonal positive matrices $P_1 \in R^{2\times 2}$ and $P_2 \in R^{2\times 2}$, we define $\Omega(x) = \mathrm{col}\{P_1(x),\ 0_{8\times 2}\}$, and

$$\Theta(x) = \begin{bmatrix} \Theta_{11} & \Theta_{12} & -rhU^\top F & rhU^\top \Gamma & 0 \\ * & \Theta_{22} & -rhF^\top F & rhF^\top \Gamma & 0 \\ * & * & \beta I & rhF^\top \Gamma & 0 \\ * & * & * & \Theta_{44} & 0 \\ * & * & * & * & \Theta_{55} \end{bmatrix}, \tag{23}$$

$$\Xi(x) = \begin{bmatrix} \Xi_{11} & -P_1(x)(F + \kappa I) & 0 & 0 & 0 \\ * & re^{-2\mu h} I + \kappa P_1(x) & 0 & 0 & 0 \\ * & * & \beta I & 0 & 0 \\ * & * & * & \Xi_{44} & 0 \\ * & * & * & * & \Xi_{55} \end{bmatrix}, \tag{24}$$

with

$$\Theta_{11} = (\mu|\Gamma| - 2\sigma I - \kappa(\lambda - 1) - U^\top)P_1(x) - (P_1(x) + rhU^\top)U,$$
$$\Theta_{12} = -(P_1(x) + rhU^\top)F - \kappa P_1(x),$$
$$\Theta_{22} = (1 - 2\sigma h) re^{-2\mu h} I - rhF^\top F + \kappa P_1(x),$$
$$\Theta_{44} = (\mu|\Gamma| - (\kappa\lambda + 2\sigma)I - M^\top)P_2(x) - P_2(x)M - rh\Gamma\Gamma,$$
$$\Theta_{55} = -\gamma((rh+1)F^\top F + \beta I) + \kappa P_2(x),$$
$$\Xi_{11} = \Theta_{11} + rhU^\top U,$$
$$\Xi_{44} = \Theta_{44} + rh\Gamma\Gamma,$$
$$\Xi_{55} = \Theta_{55} + \gamma rhF^\top F,$$

where $P_1(x) = \mathtt{diag}\{e^{\mu(L-x)}, e^{\mu x}\}P_1$, $P_2(x) = \mathtt{diag}\{e^{\mu(L-x)}, e^{\mu x}\}P_2$, $\gamma = \bar{b}^2/\pi^2$, $\lambda > 1$, $\sigma < \frac{1}{2h}$, μ, β, r, κ are positive scalars.

We then have the following main result.

Theorem 1: *The mixed traffic flow system (13)-(14) under the time-gap setting of ACC-equipped vehicles (16) is exponentially stable for any sampling sequence satisfying $t_{k+1} - t_k \in (0, h]$ in H^1-norm, if there exist positive scalars r, μ, β, κ and diagonal positive matrices $P_1 \in R^{2\times 2}$ and $P_2 \in R^{2\times 2}$ such that the following inequalities hold:*

$$(i) \quad \Delta = e^{\mu L} G^\top |\Gamma| P_1 G - |\Gamma| P_1 \leq 0, \tag{25}$$

$$\digamma = \begin{bmatrix} \digamma_{11} & \Gamma G^\top |\Gamma^{-1}| P_2 A & \Gamma G^\top |\Gamma^{-1}| P_2 B \\ * & A^\top |\Gamma^{-1}| P_2 A & A^\top |\Gamma^{-1}| P_2 B \\ * & * & B^\top |\Gamma^{-1}| P_2 B \end{bmatrix} \leq 0, \tag{26}$$

with $\digamma_{11} = \Gamma G^\top |\Gamma^{-1}| P_2 G \Gamma - e^{-\mu L} |\Gamma| P_2$, $A = M_1 G + M_2 - GM_1 - GM_2 G$, $B = GH_1 + GH_2 G - H_1 G - H_2$;

$$(ii) \quad \Upsilon(0) \geq 0, \quad \Upsilon(L) \geq 0, \tag{27}$$

with $\Upsilon(x)$ defined for all $x \in [0, L]$ as

$$\Upsilon(x) = \begin{bmatrix} \Theta(x) & \Omega(x) \\ * & I \end{bmatrix};$$

$$(iii) \quad \Phi(0) \geq 0, \quad \Phi(L) \geq 0, \tag{28}$$

with $\Phi(x)$ defined for all $x \in [0, L]$ as

$$\Phi(x) = \begin{bmatrix} \Xi(x) & \Omega(x) \\ * & I \end{bmatrix}.$$

Proof: Select the Lyapunov function candidate as

$$V = V_1(\xi) + V_2(\xi_x) + V_3 \tag{29}$$

with $V_1(\xi) = \int_0^L \xi^\top P_1(x) \xi dx$, $V_2(\xi_x) = \int_0^L \xi_x^\top P_2(x) \xi_x dx$, $V_3 = \int_0^L r(t_{k+1} - t) \int_{t_k}^t e^{2\mu(s-t)} \xi_s^\top \xi_s ds dx$, where $\xi_t = \partial_t \xi$ and $\xi_x = \partial_x \xi$ for simplicity.

Here $V_1(\xi)$ is used to bound ξ, and $V_2(\xi_x)$ is used to limit the term $\xi_x(t_k)$ obtained by processing the space discretization error $\delta(x, t_k)$. V_3 is used to handle the time sampling error $\eta(x,t)$. The proof of Theorem 1 mainly relies on the analysis of estimates for the time derivatives of $V_i, i = 1, 2, 3$, along solutions of system (21)-(22), by expanding the analysis to the dynamics of ξ_t with the assumption that solutions ξ are of class C^1.

• *Analysis of the first term $V_1(\xi)$.*

Utilizing the integration by parts, the time-derivative of $V_1(\xi)$ for $\forall t \in [t_k, t_{k+1})$, along the solutions of equations (21)-(14) is calculated as

$$\begin{aligned} \dot{V}_1(\xi) = (\xi^{out})^\top \Delta \xi^{out} + \int_0^L \big[&\xi^\top (U^\top P_1(x) + P_1(x) U - \mu \\ &|\Gamma| P_1(x)) \xi + (\delta^\top + \eta^\top) F^\top P_1(x) \xi + \xi^\top P_1(x) F \\ &(\delta + \eta) \big] dx. \end{aligned} \tag{30}$$

• *Analysis of the second term $V_2(\xi_x)$.*

Under the assumption that ξ is the class of C^1, we can obtain the dynamic of ξ_x as

$$\xi_{tx} + \Gamma \xi_{xx} = M \xi_x, \quad \forall t \in [t_k, t_{k+1}), \tag{31}$$

with the boundary condition for $t \in [t_k, t_{k+1})$,

$$\xi_x^{in} = \Gamma^{-1}(G \Gamma \xi_x^{out} + A \xi^{out} + B \xi^{out}(t_k)). \tag{32}$$

Taking the time derivative of $V_2(\xi_x)$ along the solutions of system (31)-(32), $\forall t \in [t_k, t_{k+1})$, we get

$$\begin{aligned} \dot{V}_2(\xi_x) = e^{\mu L} \theta^\top \digamma \theta + \int_0^L &\xi_x^\top (M^\top P_2(x) + P_2(x) M \\ &- \mu |\Gamma| P_2(x)) \xi_x dx, \end{aligned} \tag{33}$$

where $\theta = \mathrm{col}\{\xi_x^{out}, \xi^{out}, \xi^{out}(t_k)\}$.

• *Analysis of the third term V_3.*

Computing the time derivative of V_3, $\forall t \in [t_k, t_{k+1})$, it yields that

$$\begin{aligned} \dot{V}_3 = &r(t_{k+1} - t) \int_0^L [U\xi - \Gamma \xi_x + F(\eta + \delta)]^\top [U\xi - \Gamma \xi_x \\ &+ F(\eta + \delta)] dx - r \int_0^L \int_{t_k}^t e^{2\mu(s-t)} \xi_s^\top \xi_s ds dx. \end{aligned} \tag{34}$$

For $t \in [t_k, t_{k+1})$, it follows from (30), (33) and (34) that

$$\begin{aligned} \dot{V} + 2\sigma V = &\dot{V}_1(\xi) + \dot{V}_2(\xi_x) + 2\sigma(V_1 + V_2) + r(t_{k+1} - t) \\ &\int_0^L \xi_t^\top \xi_t dx + (2\sigma(t_{k+1} - t) - 1) r \int_0^L \int_{t_k}^t \\ &e^{2\mu(s-t)} \xi_s^\top \xi_s ds dx. \end{aligned} \tag{35}$$

Considering $\sigma < \frac{1}{2h}$ and applying Jensen's inequality [14], the last term on the right-hand side of the above equation satisfies

$$\begin{aligned} &(2\sigma(t_{k+1} - t) - 1) r \int_0^L \int_{t_k}^t e^{2\mu(s-t)} \xi_s^\top \xi_s ds dx \\ &\leq (2\sigma(t_{k+1} - t) - 1) r e^{-2\mu h} \int_0^L \eta^\top \eta dx. \end{aligned} \tag{36}$$

By using Young's inequality and Wirtinger's inequality [15], it can be obtained that

$$\begin{aligned} \int_0^L \delta^\top F^\top P_1(x) \xi dx \leq &\frac{\gamma}{2} \int_0^L \xi_x^\top(t_k) F^\top F \xi_x(t_k) dx \\ &+ \frac{1}{2} \int_0^L \xi^\top P_1(x) P_1(x) \xi dx, \end{aligned} \tag{37}$$

$$\begin{aligned} \int_0^L \delta^\top (r(t_{k+1} - t) F^\top F + \beta I) \delta dx \leq \gamma \int_0^L &\xi_x^\top(t_k) (r(t_{k+1} \\ &- t) F^\top F + \beta I) \xi_x(t_k) dx. \end{aligned} \tag{38}$$

Substitute (36)-(38) into (35), and then we have

$$\dot{V} + 2\sigma V \leq e^{\mu L} \theta^\top \digamma \theta + (\xi^{out})^\top \Delta \xi^{out} + \int_0^L \phi^\top \mathcal{W}(x) \phi dx, \tag{39}$$

where $\phi = \mathrm{col}\{\xi, \eta, \delta, \xi_x, \xi_x(t_k)\}$ and

$$\mathcal{W}(x)=\begin{bmatrix} \mathcal{W}_{11} & \mathcal{W}_{12} & \mathcal{W}_{13} & -r(t_{k+1}-t)U^\top\Gamma & 0 \\ * & \mathcal{W}_{22} & \mathcal{W}_{23} & -r(t_{k+1}-t)F^\top\Gamma & 0 \\ * & * & -\beta I & -r(t_{k+1}-t)F^\top\Gamma & 0 \\ * & * & * & \mathcal{W}_{44} & 0 \\ * & * & * & * & \mathcal{W}_{55} \end{bmatrix}, \tag{40}$$

with

$$\begin{aligned}
\mathcal{W}_{11} =&(2\sigma I-\mu|\Gamma|+P_1(x)+U^\top)P_1(x)+(P_1(x)+r(t_{k+1} \\
&-t)U^\top)U, \\
\mathcal{W}_{12} =&(P_1(x)+r(t_{k+1}-t)U^\top)F, \\
\mathcal{W}_{13} =&r(t_{k+1}-t)U^\top F, \\
\mathcal{W}_{22} =&(2\sigma(t_{k+1}-t)-1)re^{-2\mu h}I+r(t_{k+1}-t)F^\top F, \\
\mathcal{W}_{23} =&r(t_{k+1}-t)F^\top F, \\
\mathcal{W}_{44} =&(2\sigma I-\mu|\Gamma|+M^\top)P_2(x)+P_2(x)M+r(t_{k+1}-t)\Gamma\Gamma, \\
\mathcal{W}_{55} =&\gamma((r(t_{k+1}-t)+1)F^\top F+\beta I).
\end{aligned}$$

Since conditions (27)-(28) hold, it follows from Lemma 1 in the Appendix I that $\mathcal{M}(0) \geq 0$ and $\mathcal{M}(L) \geq 0$. Then, by using Lemma 2 in the Appendix I, we get

$$\int_0^L \phi^\top(\mathcal{W}(x)+\kappa\mathcal{N}(x))\phi dx \leq 0, \tag{41}$$

where $\mathcal{N}(x)$ is defined in (A.4).

Considering $t \in [t_k, t_{k+1})$, we have $\lambda(V_1(\xi(t_k,\cdot))+V_2(\xi_x(t_k,\cdot)))-(V_1(\xi(t,\cdot))+V_2(\xi_x(t,\cdot))) \geq 0$ with some $\lambda > 1$. Based on the definition of $V_1(\xi)$ and $V_2(\xi_x)$, it holds that $\int_0^L \phi^\top\mathcal{N}(x))\phi dx \geq 0$. According to (41), we then have $\int_0^L \phi^\top\mathcal{W}(x)\phi dx \leq 0$. Hence, it follows from inequalities (25)-(26) that

$$\dot{V} \leq -2\sigma V. \tag{42}$$

Based on the definition of the Lyapunov function of (29), there exists a sufficiently large constant $\varrho > 0$ such that the following inequalities hold:

$$\frac{1}{\varrho}\int_0^L (|\xi|^2+|\xi_x|^2)dx \leq V \leq \varrho\int_0^L (|\xi|^2+|\xi_x|^2)dx. \tag{43}$$

Using (42) and (43) for all $t \in [0,\infty)$, we obtain that

$$\|\xi(\cdot,t)\|_{H^1((0,L);R^2)} \leq \varrho e^{-\sigma t}\|\xi^0\|_{H^1((0,L);R^2)}.$$

Consequently, if inequalities (25)-(28) are satisfied, system (13)-(14) under the time-gap setting of ACC-equipped vehicles (16) is exponentially stable in H^1-norm. This completes the proof of Theorem 1. □

IV. NUMERICAL SIMULATIONS

The purpose of this section is to validate the exponential stability conditions proposed in Theorem 1 through the numerical simulation.

We consider a road segment with length of $L = 1$ kilometer in congested regime. The traffic parameters of the mixed traffic flow model are given as $q_{in} = 3500$ veh./hr, $\rho_{min} = 50$ veh./km, $D = 5$ m, $h_m = 1$ s, $\tau_{acc} = 100$ s, $\tau_m = 200$ s, $\alpha = 0.15$, $h = 0.002$, $\bar{b} = 0.1$ km. We expect that the traffic dynamics reach to the desired values $\rho^* = 70$ veh./km, $v^* = 50$ km/hr within steady-state time gap for ACC-equipped vehicles $h^*_{acc} = 1.5$ s.

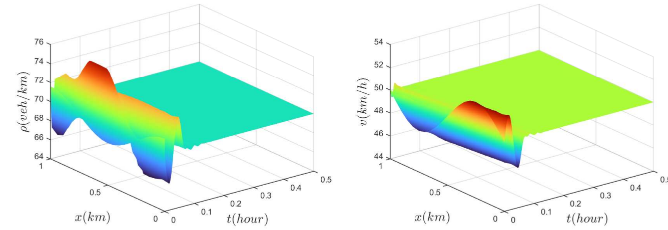

(a) (b)

Fig. 2. The evolutions of traffic dynamic of the mixed traffic flow system (13)-(14) under the time-gap setting of ACC-equipped vehicles (16). (a) The evolution of traffic density ρ; (b) The evolution of average speed v.

Choose the sampled-data distributed control gains in (16) as $k_\omega = 0.2$, $k_z = 0.13$. The parameters are selected as $k_v = 0.2$, $\mu = 0.01, \lambda = 1.3, \sigma = 0.3, \kappa = 0.01, \beta = 0.2$. By solving the conditions (25)-(28) in Theorem 1, we obtain $r = 0.0057$ and the diagonal matrices

$$P_1 = \begin{bmatrix} 3.8626 & 0 \\ 0 & 0.1039 \end{bmatrix}, P_2 = \begin{bmatrix} 0.5578 & 0 \\ 0 & 0.0792 \end{bmatrix}.$$

To compute the solutions of system (13), we discretize them by using the two-step variant of Lax-Wendroff method in [16]. The initial state associated with the steady state (ρ^*, v^*) is given as

$$\begin{cases} \rho(x,0) = \rho^* + 1.6cos(2\pi x), \\ v(x,0) = v^* + 2.4cos(2\pi x). \end{cases} \tag{44}$$

Fig. 2(a) and 2(b) show the evolutions of the traffic density $\rho(x,t)$ and the average speed $v(x,t)$ of the mixed traffic flow system (13)-(14) under the time-gap setting of ACC-equipped vehicles (16), respectively. It can be observed that both the traffic density and the average speed converge to the steady states $\rho^* = 70$ veh./km, $v^* = 50$ km/hr within the time-gap setting of ACC-equipped vehicles $h^*_{acc} = 1.5$ s. As revealed in the above results, the inequality conditions provided in Theorem 1 are validated for ensuring the exponential convergence of the mixed traffic flow.

V. CONCLUSIONS

This paper has addressed the sampled-data distributed control problem for mixed traffic flow with ACC-equipped vehicles in H^1-norm. The time-gap setting of ACC-equipped vehicles is designed based on the spatially sampled state measurements provided by the sensors to drive the traffic dynamic to the steady state. By re-modeling the closed-loop system into an equivalent system with spatio-temporal sampling errors and using the Lyapunov function approach, we have derived sufficient conditions for ensuring the exponential stability of the mixed traffic flow system.

Appendix I
Some useful Lemmas

Lemma 1: If the conditions (27) and (28) hold, then

$$\mathcal{M}(0) \geq 0,\ \mathcal{M}(L) \geq 0, \tag{A.1}$$

with $\mathcal{M}(x)$ defined for all $x \in [0, L]$ as

$$\mathcal{M}(x) = \begin{bmatrix} Q(x) & \Omega(x) \\ * & I \end{bmatrix}, \tag{A.2}$$

where

$$Q(x)=\begin{bmatrix} Q_{11} & Q_{12} & Q_{13} & r(t_{k+1}-t)U^{\top}\Gamma & 0 \\ * & Q_{22} & Q_{23} & r(t_{k+1}-t)F^{\top}\Gamma & 0 \\ * & * & \beta I & r(t_{k+1}-t)F^{\top}\Gamma & 0 \\ * & * & * & Q_{44} & 0 \\ * & * & * & * & Q_{55} \end{bmatrix},$$

with

$$\begin{aligned} Q_{11} &= (\mu|\Gamma|-2\sigma I-\kappa(\lambda-1)-U^{\top})P_1(x)-(P_1(x)+r(t_{k+1} \\ &\quad -t)U^{\top})U, \\ Q_{12} &= -(P_1(x)+r(t_{k+1}-t)U^{\top})F-\kappa P_1(x), \\ Q_{13} &= -r(t_{k+1}-t)U^{\top}F, \\ Q_{22} &= (1-2\sigma(t_{k+1}-t))re^{-2\mu h}I-r(t_{k+1}-t)F^{\top}F+\kappa P_1(x), \\ Q_{23} &= -r(t_{k+1}-t)F^{\top}F, \\ Q_{44} &= (\mu|\Gamma|-(\kappa\lambda+2\sigma)I-M^{\top})P_2(x)-P_2(x)M-r(t_{k+1} \\ &\quad -t)\Gamma\Gamma, \\ Q_{55} &= -\gamma((r(t_{k+1}-t)+1)F^{\top}F+\beta I)+\kappa P_2(x). \end{aligned}$$

Proof: According to the definitions of $\Upsilon(0)$ and $\Phi(0)$, it yields that

$$\varsigma(t)\Upsilon(0)+\frac{t-t_k}{t_{k+1}-t_k}\Phi(0)=\begin{bmatrix} \Pi & \Omega(0) \\ * & I \end{bmatrix}, \tag{A.3}$$

where $\varsigma(t) = \frac{t_{k+1}-t}{t_{k+1}-t_k}$ and

$$\Pi=\begin{bmatrix} \Pi_{11} & \Pi_{12} & \Pi_{13} & \varsigma(t)rhU^{\top}\Gamma & 0 \\ * & \Pi_{22} & \Pi_{23} & \varsigma(t)rhF^{\top}\Gamma & 0 \\ * & * & \beta I & \varsigma(t)rhF^{\top}\Gamma & 0 \\ * & * & * & \Pi_{44} & 0 \\ * & * & * & * & \Pi_{55} \end{bmatrix},$$

with

$$\begin{aligned} \Pi_{11} &= (\mu|\Gamma|-2\sigma I-\kappa(\lambda-1)-U^{\top})P_1(0)-(P_1(0)+\varsigma(t)rhU^{\top})U, \\ \Pi_{12} &= -(P_1(0)+\varsigma(t)rhU^{\top})F-\kappa P_1(0), \\ \Pi_{13} &= -\varsigma(t)rhU^{\top}F, \\ \Pi_{22} &= (1-2\sigma\varsigma(t)h)re^{-2\mu h}I-\varsigma(t)rhF^{\top}F+\kappa P_1(0), \\ \Pi_{23} &= -\varsigma(t)rhF^{\top}F, \\ \Pi_{44} &= (\mu|\Gamma|-(\kappa\lambda+2\sigma)I-M^{\top})P_2(0)-P_2(0)M-\varsigma(t)rh\Gamma\Gamma, \\ \Pi_{55} &= -\gamma((\varsigma(t)rh+1)F^{\top}F+\beta I)+\kappa P_2(0). \end{aligned}$$

The feasibility of $\Upsilon(0) \geq 0$ and $\Phi(0) \geq 0$ guarantee $\varsigma(t)\Upsilon(0)+\frac{t-t_k}{t_{k+1}-t_k}\Phi(0) \geq 0$. Since $\frac{h}{t_{k+1}-t_k} \geq 1$, it can be easily obtained that $\mathcal{M}(0) \geq 0$.

Following the similar arguments, we have that $\Upsilon(L) \geq 0$ and $\Phi(L) \geq 0$ ensure $\varsigma(t)\Upsilon(L)+\frac{t-t_k}{t_{k+1}-t_k}\Phi(L) \geq 0$, which implies $\mathcal{M}(L) \geq 0$.

This concludes the proof of Lemma 1.

Lemma 2: If the conditions $\mathcal{M}(0) \geq 0$ and $\mathcal{M}(L) \geq 0$ hold, then $\mathcal{W}(x) + \kappa\mathcal{N}(x) \leq 0$, $\forall x \in [0, L]$, where

$$\mathcal{N}(x)=\begin{bmatrix} (\lambda-1)P_1(x) & P_1(x) & 0 & 0 & 0 \\ * & -P_1(x) & 0 & 0 & 0 \\ * & * & 0 & 0 & 0 \\ * & * & * & \lambda P_2(x) & 0 \\ * & * & * & * & -P_2(x) \end{bmatrix}. \tag{A.4}$$

Proof: If $\mathcal{M}(0) \geq 0$ and $\mathcal{M}(L) \geq 0$ hold, we have $\mathcal{M}(x) \geq 0$ for $x \in [0, L]$. According to the Schur complement [17] and the definition of $\mathcal{M}(x)$ in (A.2), it can be obtained that $Q(x) - \Omega(x)I\Omega^{\top}(x) \geq 0$, which is equivalent to $Q(x) - \bar{\Omega}(x)I\bar{\Omega}^{\top}(x) \geq 0$, where $\bar{\Omega}(x) = [\,\Omega(x) \quad 0_{10\times 8}\,]$. The above inequality can be re-expressed as $\mathcal{W}(x) + \kappa\mathcal{N}(x) \leq 0$, for all $x \in [0, L]$.

This concludes the proof of Lemma 2.

References

[1] A. Aw and M. Rascle. Resurrection of "second order" models of traffic flow. *SIAM Journal on Applied Mathematics*, 60(3):916–938, 2000.

[2] H. M. Zhang. A non-equilibrium traffic model devoid of gas-like behavior. *Transportation Research Part B*, 36(3):275–290, 2002.

[3] L. Zhang, H. Luan, Y. Lu, and C. Prieur. Boundary feedback stabilization of freeway traffic networks: ISS control and experiments. *IEEE Transactions on Control Systems Technology*, 30(3):997–1008, 2021.

[4] H. Yu and M. Krstic. Traffic congestion control for Aw-Rascle-Zhang model. *Automatica*, 100:38–51, 2019.

[5] H. Zhao, J. Zhan, and L. Zhang. Saturated boundary feedback control of LWR traffic flow models with lane-changing. *IEEE 61st Conference on Decision and Control (CDC)*, pages 838–843, 2022.

[6] A. Spiliopoulou, D. Manolis, F. Vandorou, and M. Papageorgiou. Adaptive cruise control operation for improved motorway traffic flow. *Transportation Research Record*, 2672(22):24–35, 2018.

[7] J. Yi and R. Horowitz. Macroscopic traffic flow propagation stability for adaptive cruise controlled vehicles. *Transportation Research Part C: Emerging Technologies*, 14(2):81–95, 2006.

[8] N. Bekiaris-Liberis and A I. Delis. PDE-based feedback control of freeway traffic flow via time-gap manipulation of ACC-equipped vehicles. *IEEE Transactions on Control Systems Technology*, 29(1):461–469, 2020.

[9] L. Hetel, C. Fiter, H. Omran, A. Seuret, E. Fridman, J.-P. Richard, and S. I. Niculescu. Recent developments on the stability of systems with aperiodic sampling: An overview. *Automatica*, 76:309–335, 2017.

[10] E. Fridman and N. B. Am. Sampled-data distributed H_∞ control of transport reaction systems. *SIAM Journal on Control and Optimization*, 51(2):1500–1527, 2013.

[11] I. Karafyllis and M. Krstic. Sampled-data boundary feedback control of 1-d parabolic PDEs. *Automatica*, 87:226–237, 2018.

[12] N. Espitia, A. Girard, N. Marchand, and C. Prieur. Event-based control of linear hyperbolic systems of conservation laws. *Automatica*, 70:275–287, 2016.

[13] X. Wang, Y. Tang, C. Fiter, and L. Hetel. Sampled-data distributed control for homo-directional linear hyperbolic system with spatially sampled state measurements. *Automatica*, 139:110183, 2022.

[14] K. Gu, V. Kharitonov, and J. Chen. *Stability of Time-Delay Systems*. Birkhauser, Boston, 2003.

[15] K. Liu, V. Suplin, and E. Fridman. Stability of linear systems with general sawtooth delay. *IMA Journal of Mathematical Control and Information*, 27(4):419–436, 2010.

[16] L. Shampine. Solving hyperbolic PDEs in matlab. *Appl. Numer. Anal. Comput. Math*, 2:346–358, 2005.

[17] S. Boyd, L. E. Ghaoui, E. Feron, and V. Balakrishnan. *Linear matrix inequalities in system and control theory*. SIAM journal on applied mathematics, 1994.